

Biomimetic Hairy Whiskers for Robotic Skin Tactility

Jie An, Pengfei Chen, Ziming Wang, Andy Berbille, Hao Pang, Yang Jiang, Tao Jiang,* and Zhong Lin Wang*

Touch sensing is among the most important sensing capabilities of a human, and the same is true for smart robotics. Current research on tactile sensors is mainly concentrated on electronic skin (e-skin), but e-skin is prone to be easily dirtied, damaged, and disturbed after repeated usage, which greatly limits its practical applications in robotics. Here, by mimicking the way that animals explore the environment using hair-based sensors, a bendable biomimetic whisker mechanoreceptor (BWMR) is designed for robotic tactile sensing. Owing to the advantages of triboelectric nanogenerator technology, the BWMR can convert external mechanical stimuli into electrical signals without a power supply, which is conducive to its widespread applications in robots. Because of the leverage effect of the whisker, the BWMR can distinguish an exciting force of 1.129 μN by amplifying external weak signals, which can be further improved by increasing the whisker length. Real-time sensing is demonstrated using a BWMR, exhibiting its potential for robotic tactile systems.

obstacles, and explore confined space under low visibility condition. Therefore, it is not enough to rely solely on visual sensors, and seeking supplementary and complementary sensing strategies is essential to expand the application fields and adaptability of intelligent robots.^[3]

In Nature, there are many creatures living in dark, narrow, turbid, and other extreme environments. They can understand their environment and identify and capture prey using the sense of touch.^[4] Their environmental adaptation strategies can be imitated by humans to solve information detection problems in similar extreme conditions. These creatures are all endowed using sensors with similar structures, that is, there is an obvious feeler rod or protrusion, such as the lateral lines of fishes^[3] and the hairy whiskers of pinnipeds and rodents.^[5] They can receive external fluid signals or collision signals by sensing the strain of probe rod. Inspired by nature, a biomimetic whisker mechanoreceptor based on triboelectric nanogenerator (TENG) technology can be designed.

The tentacle detectors have been invented for many years, mainly used for remote operated vehicle and amphibious robots to rescue, detect pollutants, and explore turbid water environments. However, the traditional tactile detectors are mainly based on the principles of piezoresistance, piezoelectricity, optics, and magnetism.^[3,6] These sensors have their own shortcomings, such as large energy consumption even at non-working state,^[7] and heavy, susceptible-to-interference, high-cost, and difficult to miniaturize, array and package, which hinders the widespread application of these technologies in robotics field. However, the TENG-based technology with advantages of light weight, easy fabrication, low-cost, diverse material selection and simple structure, etc.^[8] provides a new strategy for developing a self-powered BWMR.

Recently, the TENG was invented as a new electromechanical conversion technology,^[9] which can not only be used in energy harvesting,^[10] but also as an excellent self-powered electromechanical sensor,^[11] due to its high sensitivity to mechanical stimuli. Abundant TENG-based sensors, such as vibration,^[12] sound,^[11e,13] liquid level,^[14] angle,^[15] and touch sensors,^[11c,d] have emerged. However, traditional data acquisition circuit cannot be matched with them due to the capacitive impedance of TENGs, which is the main limitation to the commercial availability of TENG-based sensors.^[11b-d] In addition to that, most of the previous efforts in the development of tactile technologies have focused on electronic skin,^[11d,16] while relatively fewer

1. Introduction

Animals have many different forms of physical senses to perceive the external environment, such as sight, hearing, smell, taste, and touch. By imitating the principle of animal vision, current robots acquire external information mainly relying on video cameras and image recognition technology.^[1] However, with the rapid development of computers, microelectronics, and information processing technologies, higher requirements are put forward for them to sense environmental information more accurately and quickly as a human,^[2] which is vital for their applications in uncertain and complex conditions. For instance, they are required to be able to safely navigate, avoid

J. An, P. Chen, Z. Wang, A. Berbille, H. Pang, Y. Jiang, Prof. T. Jiang, Prof. Z. L. Wang
CAS Center for Excellence in Nanoscience
Beijing Institute of Nanoenergy and Nanosystems
Chinese Academy of Sciences
Beijing 100083, China
E-mail: jiangtao@binn.cas.cn; zlwang@gatech.edu

J. An, P. Chen, Z. Wang, A. Berbille, Y. Jiang, Prof. T. Jiang, Prof. Z. L. Wang
School of Nanoscience and Technology
University of Chinese Academy of Sciences
Beijing 100049, China
Prof. Z. L. Wang
School of Materials Science and Engineering
Georgia Institute of Technology
Atlanta, GA 30332-0245, USA

 The ORCID identification number(s) for the author(s) of this article can be found under <https://doi.org/10.1002/adma.202101891>.

DOI: 10.1002/adma.202101891

works have been carried out for the development of battery-free electronic whiskers for environmental perception.

Here, we report an easy-to-fabricate, highly sensitive, and self-powered BWMR sensor, as well as a signal acquisition circuit based on electrometer principle to construct a tactile sensing system for robotics and industry applications. The weak signals can be amplified by leverage effect of whisker and sensed by hair follicle of BWMR, exhibiting an ultrahigh sensitivity to an external stimulus, down to 1.129 μN . A tactile sensing system based on BWMR have been equipped on different parts of robots, demonstrating its function in robotics for environmental recognition, object surface topography collection, surrounding object and ground environment detection, and self-gait analysis. After signal processing by artificial intelligence, machine recognition, and other information processing technologies, the robot can acquire extraordinary tactile navigation ability and strong environmental adaptability. Furthermore, the BWMR function as a reliable, low-cost, energy-efficient, and durable mechatronic indicator is also demonstrated for parameter indication and sensing in many industrial equipment. It can solve the problem on the connection of traditional mechanical indicators to the electronic control system, which is the foundation of artificial intelligence and big data analysis. This work demonstrates versatile application of BWMR and exhibits great application foreground of TENG-based sensors for meeting the requirements of robots in terms of high adaptability to extreme environments.

2. Results and Discussion

2.1. Mechanism of Biomimetic Whisker Mechanoreceptor

Rodents like mice can roam freely in dark and narrow caves, mainly relying on their tactile system composed of hairy whisker mechanoreceptors, transmission nerves, and brain (Figure 1a). Owing to the leverage effect, the whisker can amplify the weak touch signals, which provides the mice a sensitive tactile perception.^[17] The BWMR is inspired by the sensing principle of rodents' whiskers. In order to simplify the device structure for miniaturization and integration, and ensure signal stability, a planar BWMR was first designed to detect the swing motion of the whisker in one dimension. The device consists of a 0.2 mm-thick fluorinated ethylene propylene (FEP) strip, similar to the animal whiskers, and a biomimetic hair follicle covered with two metal electrodes, acting like the sensory nerves of animal hair follicles to sense the deformation of biomimetic whisker (Figure 1b). To enhance the output signal intensity of the BWMR, the whisker surface nanostructures were prepared by the inductively coupled plasma (ICP) etching. The best contour of the inner wall of the biomimetic whisker follicle was determined through simulation analyses in order to ensure that the whisker can contact well with it to realize effective contact electrification during the swing process of whisker (Figure S1 and S2 and Note S1, Supporting Information). The biomimetic hair follicle encapsulates two electrodes of TENG, which is beneficial for resisting the interference from external environment. Such simple structure and self-powered characters are conducive to its widespread distribution on robots. Equipped with BWMR

arrays, robots can communicate with other robots, and perceive the external environment. Moreover, the objects hidden by flexible cloths or fabrics is difficult to be discovered by solely relying on vision, ultrasonic radar, and other traditional environmental detection approaches; tactile perception can help robots recognize them and obtain their outline by touch detection, which greatly expands the robots' ability to collect information on the surrounding environment (Figure 1c).

The working principle of the BWMR is based on the coupling of contact electrification and electrostatic induction. As a good electret material, the surface of FEP can carry negative charges for a long time, and these charges can also be continuously replenished during the contact process with the metal electrodes.^[18] The negatively charged FEP can cause the transfer of free charges between two electrodes during the swing process of whisker, which is dominated by the Wang term in the Maxwell's displacement current.^[19]

$$\frac{\partial \bar{D}}{\partial t} = \epsilon \frac{\partial \bar{E}}{\partial t} + \frac{\partial \bar{P}_s}{\partial t} \quad (1)$$

where \bar{P}_s is the polarization induced by the surface electrostatic charges. At the initial vertical state of the whisker, the potentials at two electrodes are equivalent. When the whisker swings to the right-hand under an external force, the root of the whisker will move toward the left-hand electrode under the action of the leverage effect, breaking the potential balance between two electrodes and driving the positive charges to flow from the right to the left electrode. The generated positive signals can be acquired by an electrometer circuit. When the whisker deflects leftward, the positive charges at the left electrode will flow back, producing negative electric signals. The working mode of the BWMR is confirmed through finite element simulations, reflected by the potential distributions at different whisker states in cross section as shown in Figure 1d. The deflection direction and amplitude of the whisker can be obtained from the signs and magnitude of the transferred charges, respectively. If the BWMRs are arrayed on the robot, the electrical signals can be acquired by a charge collection circuit and processed by a microprogrammed control unit (MCU) to realize the robot's all-round environmental detection. Meanwhile, the detected signals can be also transmitted to a central brain through WIFI, which can dispatch the robot clusters in a unified manner, and realize the coordination and cooperation between robots by analyzing the collected data (Figure 1e).

2.2. Stability Characterization of Biomimetic Whisker Mechanoreceptor for Position Sensing

When the BWMR slides across a scale ruler in the forward and backward directions, positive and negative voltage peaks can be, respectively, generated. According to the numbers of these positive and negative peaks, the direction of the movement of the BWMR and the travel distance can be acquired in order to realize the detection and measurement of the angle and displacement (Figure 2a). Figure 2b shows the profiles of open-circuit voltage (V_{OC}) and dV/dt when the BWMR slides for 100 mm forward and backward along the ruler with a pitch scale of 10 mm for two cycles. The dV/dt peaks represent the sudden change of V_{OC} , corresponding to the separation between the whisker and a

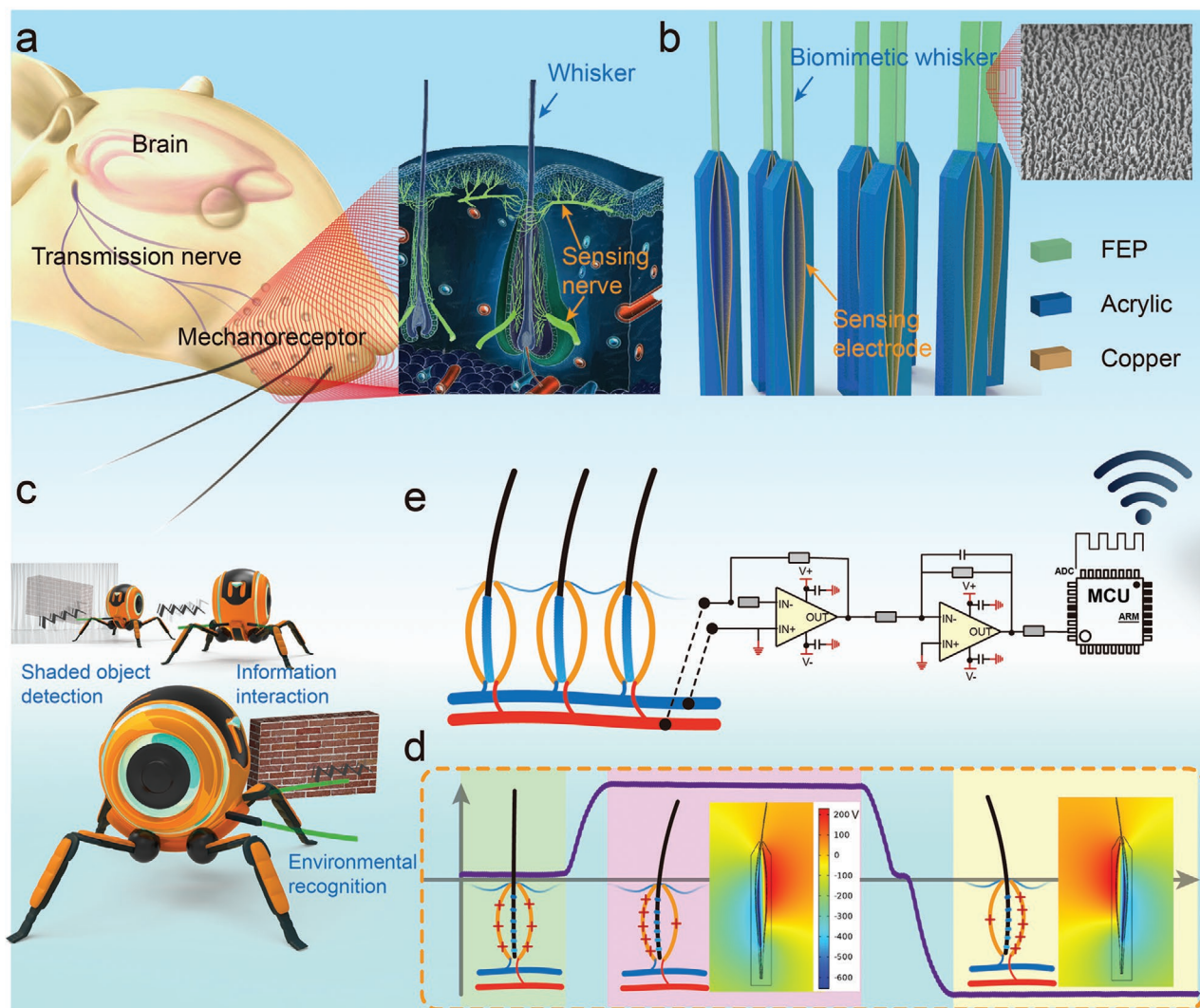


Figure 1. Bionic concept, application, and principle of the biomimetic whisker mechanoreceptor. a) Schematic illustration of animal whisker sensory system and the local anatomy of whisker mechanoreceptor. b) Schematic diagram of the structure design of the BWMR. c) Application of the BWMRs in shaded object detection, information interaction, and environment recognition for robotics. d) Schematic diagram of the acquired signals by charge acquisition circuit for the BWMR at different whisker states. e) An artificial whisker system consisting of a BWMR array, a charge acquisition circuit, an MCU, and a wireless transmitting circuit.

scale. The value difference between positive and negative signal comes from the residual stress of whisker, which bends the whisker and causes the elasticity difference when it swings forward and backward. The voltage signals have a very good periodicity, and the amplitudes of the positive and negative peaks do not fluctuate too much, even though the sensor slides back and forth at different speeds (Figure 2c). The excellent stability of the device lays the foundation for future industrial applications.

Subsequently, comprehensive experiments of voltage signal acquisition and analysis at different moving speeds of the BWMR were carried out. As presented in Figure 2d and Figure S3, Supporting Information, an identical number of voltage peaks are obtained when the sensor moves on the same distance at different speeds. The distance between two adjacent signal peaks corresponds to a moving distance of 10 mm, the distance between two scales. By counting the number of peaks in the voltage signals, the real-time position of the BWMR can be acquired. As illustrated in Figure 2e, the measured position almost coincides

with the actual position curve with an associated margin of error of only 2% (Figure S4 and Note S2, Supporting Information). The measurement error cannot accumulate with the increase of the moving distance, confirming the device accuracy. Furthermore, the real-time variation of its moving velocity can be calculated through dividing the displacement by the duration of the movement. A comparison between the measured velocities (colored points) and the preset velocities (dotted lines), for different speed values, is illustrated in Figure 2f. The experimental results showed a good accuracy of the velocity measurements.

Increasing the scale density is an effective approach to improve the resolution for meeting higher accuracy requirement in some applications. Therefore, the variation of resolution at different scale densities was studied while maintaining the speed value at 10 mm s^{-1} and moving along a distance of 100 mm. The increase in scale density significantly increases the peak number of voltage signals generated by the device (Figure 2g). As the scale is reduced to 6 mm, the minimum measurement resolution is improved up

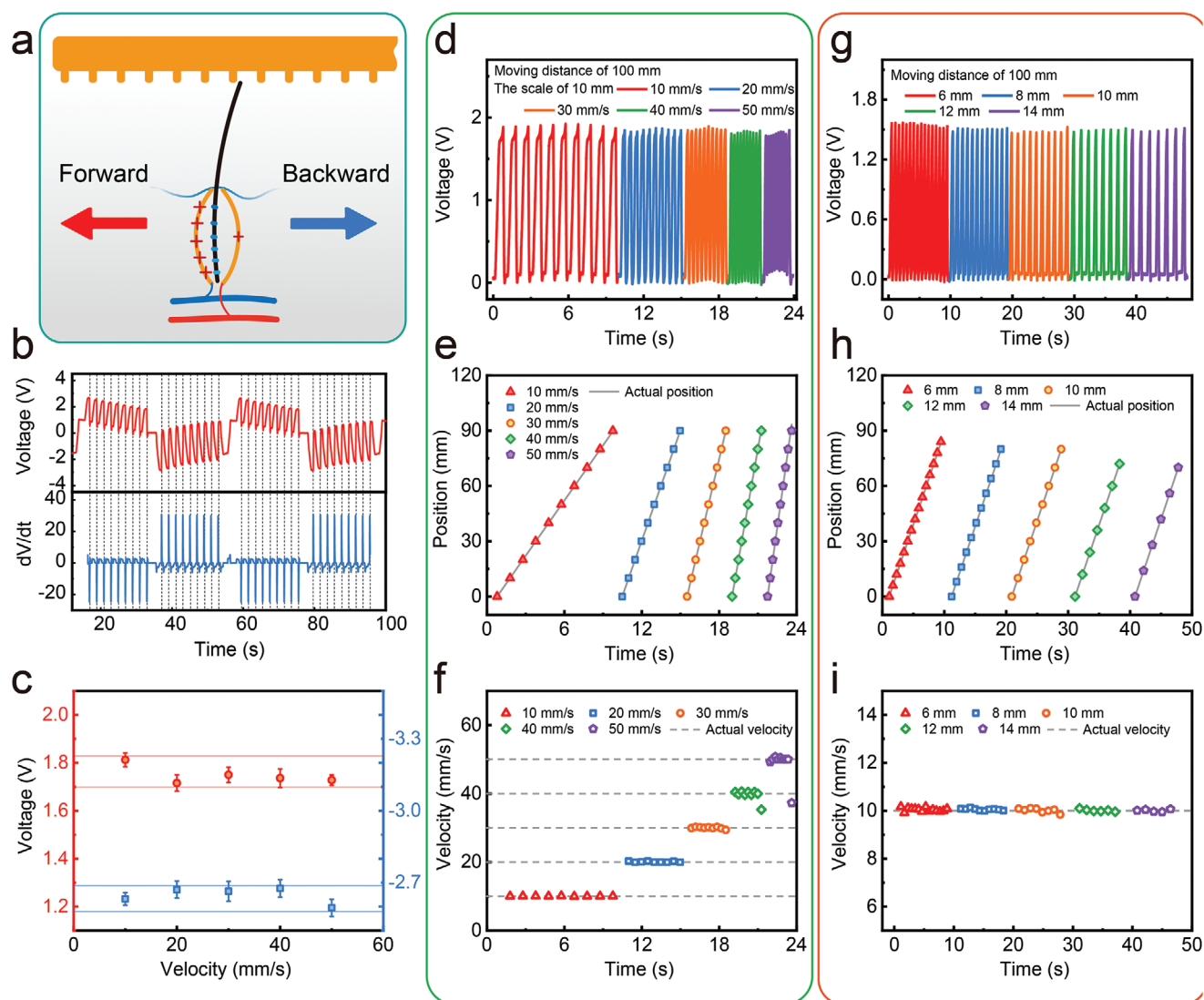


Figure 2. Electrical characteristics of the BWMR under external stimulation. a) Schematic illustration of forward and backward stimulation application. b) Open-circuit voltage (V_{OC}) and the corresponding dV/dt signals as the whisker slides across a scale ruler in two cycles of a forward and reverse scan process. c) Amplitude variation of V_{OC} at different scan speeds. The red and blue dots denote the voltage amplitudes during forward and backward scan processes, respectively. d) V_{OC} of the BWMR when scanning forward at different speeds (the scan distance is 100 mm and the scale is 10 mm). e) Calculated displacements and f) real-time velocities according to the signal peak numbers in (d), compared with actual values at different scan speeds. g) V_{OC} of the BWMR when scanning forward at the same speed for different densities of scale. h) Calculated displacements and i) real-time velocities from (g), compared with the actual values.

to 6 mm accordingly. The measured position and velocity completely coincide with the actual lines for all scale densities with errors of maximum 1.66% and 1.69%, respectively (Figure 2h,i and Figure S5, Supporting Information), thus demonstrating that the measurement accuracy will not be affected by reducing the scale distance. This approach represents a simple and feasible mean to improve resolution in displacement sensing applications.

2.3. Performance Characterization of Biomimetic Whisker Mechanoreceptor for Pressure Sensing

Pressure sensitivity of the BWMR is an important characteristic for robot environmental exploration. As we all know, the

protruding whisker can produce large deformation even under weak disturbances thanks to the leverage effect, and the V_{OC} is related to the deformation of the BWMR. Therefore, according to the variations of voltage magnitude, weak signals in the environments can be harvested. The length of the whisker (L) and the position at which the force is applied (D) determine the maximum force that can be applied to the whisker (Figure 3a). The increase of D and decrease of L will improve the maximum force applied to the whisker and the maximum output voltage of BWMR correspondingly until saturation (Figure 3b and Figure S6, Supporting Information).

Application of a periodic pressure to the whisker ($D = 5$ mm, $L = 30$ mm) is shown in Figure 3c. Gradually increasing the pressure on the whisker results in a gradual enhancement of

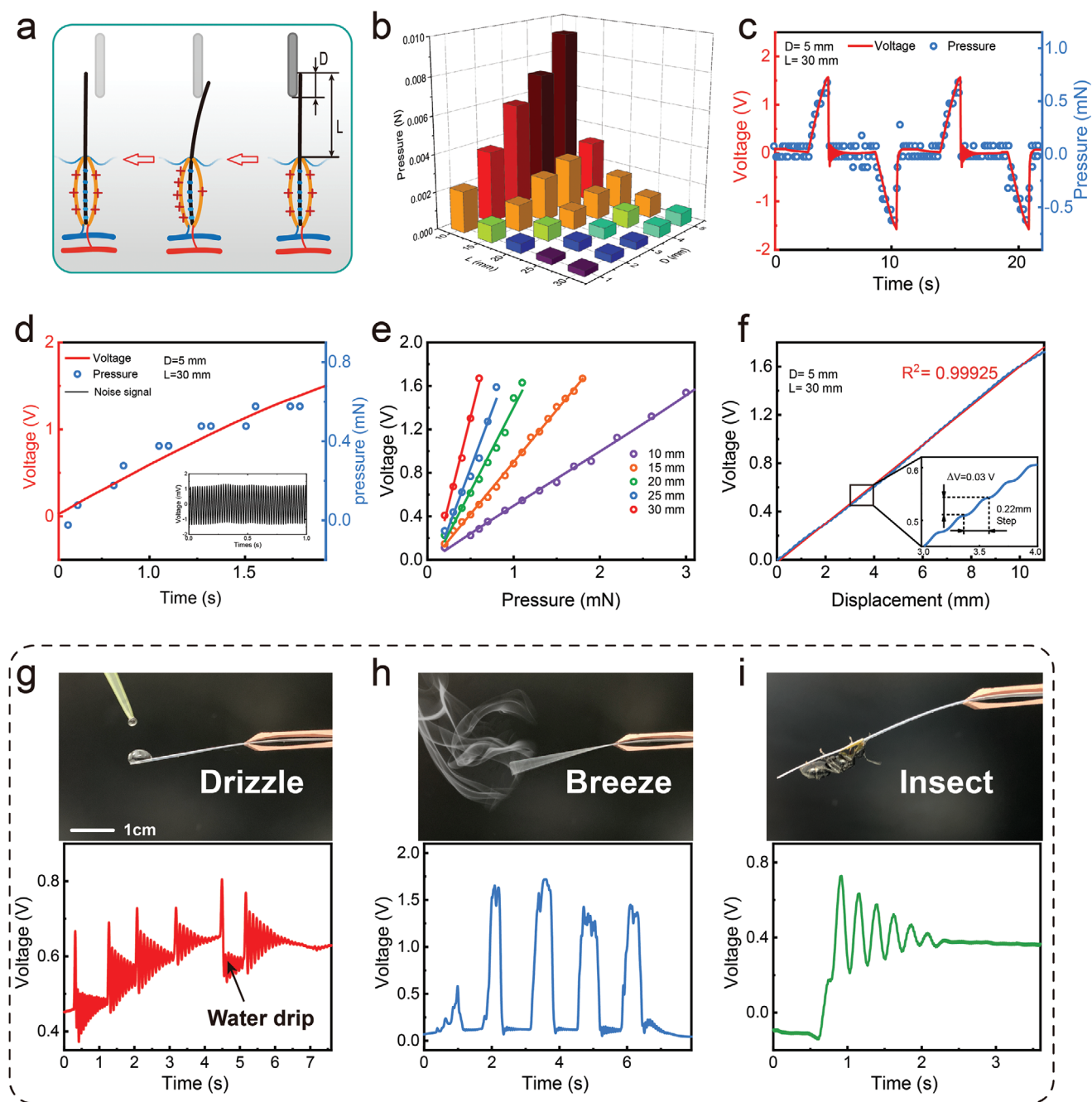


Figure 3. Corresponding characteristics of the BWMR when bearing a stimulus force. a) Schematic illustration of applying pressure to the BWMR. The whisker length, L , and contact length, D , determine the maximum pressure applied on the whisker. b) Relationship between the maximum applied pressure and the whisker length, L , as well as the contact length, D . The shorter L and the longer D produce the larger applied pressure. c) Real-time V_{OC} of the BWMR when a periodic force is applied on the whisker. The applied pressure is measured in real time by a commercial pressure sensor with a resolution of 0.1 mN. d) Sensitivity comparison between the BWMR and commercial sensors for pressure sensing. The inset is the waveform of noise signal. According to the amplitude of noise signal and V_{OC} of the BWMR, the minimum resolution can be calculated to be 1.129 μN . e) Linear relationship between the V_{OC} and pressure for different L . f) Variation of V_{OC} with increasing the displacement of whisker tip. g–i) Voltage responses of the BWMR to weak environmental disturbances, such as drizzle (g), breeze (h), and insect crawling (i).

the output voltage. When the pressure reaches the maximum value, the whisker separates from the force-applying object, and the pressure and V_{OC} drop to zero simultaneously. When the pressure is reversed, negative pressure and output voltage will be generated. Although we have used a high-performance

pressure gauge, the measured pressure values still have large fluctuations during the pressure-applying process, since the resolution and sampling rate are not high enough. However, the signals obtained by the BWMR sensor have a higher signal-to-noise ratio by contrast, which demonstrates the

superiority of the BWMR sensor for measuring weak force signals (Figure 3d). The output voltage corresponding to a pressure of 0.7 mN is 1.55 V for the BWMR ($D = 5$ mm, $L = 30$ mm), and the voltage noise in the environments is 2.5 mV (inset of Figure 3d), thus the minimum resolution R_{\min} of the BWMR for pressure sensing can be calculated by

$$R_{\min} = \frac{0.7 \text{ mN}}{1.55 \text{ V}} \times 2.5 \text{ mV} = 1.129 \mu\text{N},$$
 according to the linear

relationship between the applied pressure on the whisker and the generated V_{OC} of BWMR sensor for different whisker lengths, L (Figure 3e). Owing to the leverage effect induced amplification, the longer the whisker, the smaller the force that can be detected. Thus, the minimum resolution can be further improved by increasing the whisker length, L .

According to $F = kX$, the hypothesis that the V_{OC} is linked by a linear relationship to the swing amplitude X of the force-applied point on the whisker can be made, since the V_{OC} is proportional to the applied pressure, F . After linear fitting of the experimental results (the red line in Figure 3f), the linearity reaches 0.99925. Since the force-applying object is driven by a stepper motor with a step value of 0.22 mm, the V_{OC} generated by the BWMR will experience a stepwise increase during the force application process as illustrated in the inset of Figure 3f. Such small displacement change can also be recorded by the BWMR sensor. The good response demonstrated by the BWMR sensor to weak signals makes it a very suitable device for monitoring weak disturbances in the environments, such as drizzle, breeze, and insect crawling (Figure 3g–i).

2.4. Application in Robotics for Environment Recognition

With the development of artificial intelligence technology, the robot technology has entered a new stage. Especially in the field of image recognition, artificial intelligence has given the robots super-strong logical analysis abilities, which enables them to respond reasonably to complex situations. At present, the application fields of robots are expanding with increasing types and improved performance, and gradually developing toward intellectualization. However, in order to be capable of dealing with unknown, unpredictable, and complex environments, intelligent robots are required to be equipped with many sensory abilities, similar to animals (Figure S7, Supporting Information). Although most of the external environment information can be acquired by visual sensors, it is restricted in troubled water or narrow channels. The information acquiring method through radar scan can sometimes make up for some shortages of vision, but it may expose the positions of the robots and lead to a high energy consumption.^[3,6b]

As a kind of biomimetic sensor, the BWMR will endow the robots with tactile perception ability to explore the environments by touch like rodents, and also to track targets or avoid dangers by sensing the disturbance of the current like seals, making up for the shortages of vision and radar scan. Here, we construct an automated guided vehicle (AGV) with a tactile perception system to demonstrate the behavior of the robot in an environment exploration scenario. The tactical perception system consists of two BWMR sensors distributed on both sides

of the AGV, an electrometer data acquisition (DAQ) board used for acquiring and processing the signals from BWMRs, and a motor control circuit board for driving the motion of AGV (Figure 4a). The information interaction process of each part is shown in Figure 4b. When the AGV touches the surrounding objects during the exploring process, the charge transfer occurs between the two electrodes of the BWMR. The electrometer DAQ board collects the transferred charge signal in real time and sends it to the computer program via wireless transmission such as WIFI or Bluetooth (Figure S8 and Note S3, Supporting Information). The computer program obtains the deformation information of the whisker according to the linear relationship between the amount of transferred charge and the deformation (Figure 2f and Note S4, Supporting Information), and then controls the AGV to make appropriate actions to realize the unified control of the robot cluster. Undoubtedly, the AGV can be also directly controlled by the electrometer DAQ board to automatically perform tasks by itself.

Here, we demonstrate the ability of automatic obstacle avoidance for the AGV equipped with a tactile sensor system (Figure 4c and Video S1, Supporting Information), which is the basis for robots to achieve autonomous navigation. By analyzing the signals of the BWMRs in real time the collision angle θ can be obtained according to the equation of $\angle\theta = \arctan(d/s)$ (inset of Figure 4c and Note S5, Supporting Information); the computer program can control the AGV relying on the collision angle to realize accurate automatic obstacle avoidance (Figure 4d). The acquired transferred charge signals from two BWMR sensors during the obstacle avoidance process are shown in Figure 4e. When the sensor detects the collision signals, the robot will quickly make obstacle avoidance actions, and the sensor will return to the initial state, so the two groups of signals rise first and then quickly fall back.

Relying on tactile perception system, the robot can also recognize the surface topography and texture of touched objects. When the AGV sweeps across the object surface, the original surface topography information can be acquired by the BWMR (Figure 4f,g). Through data analysis techniques such as pseudo Wigner–Ville transformation (Figure 4h), the surface topography information and the vibration information during the movement can be distinguished easily. What's more, through analyzing the relationship between electrical signals and the moving distance of the robot, the characteristics of the object (stiff or soft) can be initially perceived. Thus, the outline of an object blocked by a soft cloth can be easily recognized, which is difficult by vision.

2.5. Application in Robotics for Vibration Detection and Road Condition Perception

In nature, there are many creatures that use tactile sensors on their legs to perceive the environment. In order to mimic their remarkable ability, we constructed a quadruped robot equipped with BWMRs on its legs, and the electrometer DAQ board acts as its body for real-time acquiring of the pressure signal from feet (Figure 5a). BWMR is especially suitable for micro robots for foot pressure detecting with high resolution, wear and impact resistance, and easy fabrication. Because wide broadband vibration in the environment can be captured by BWMR

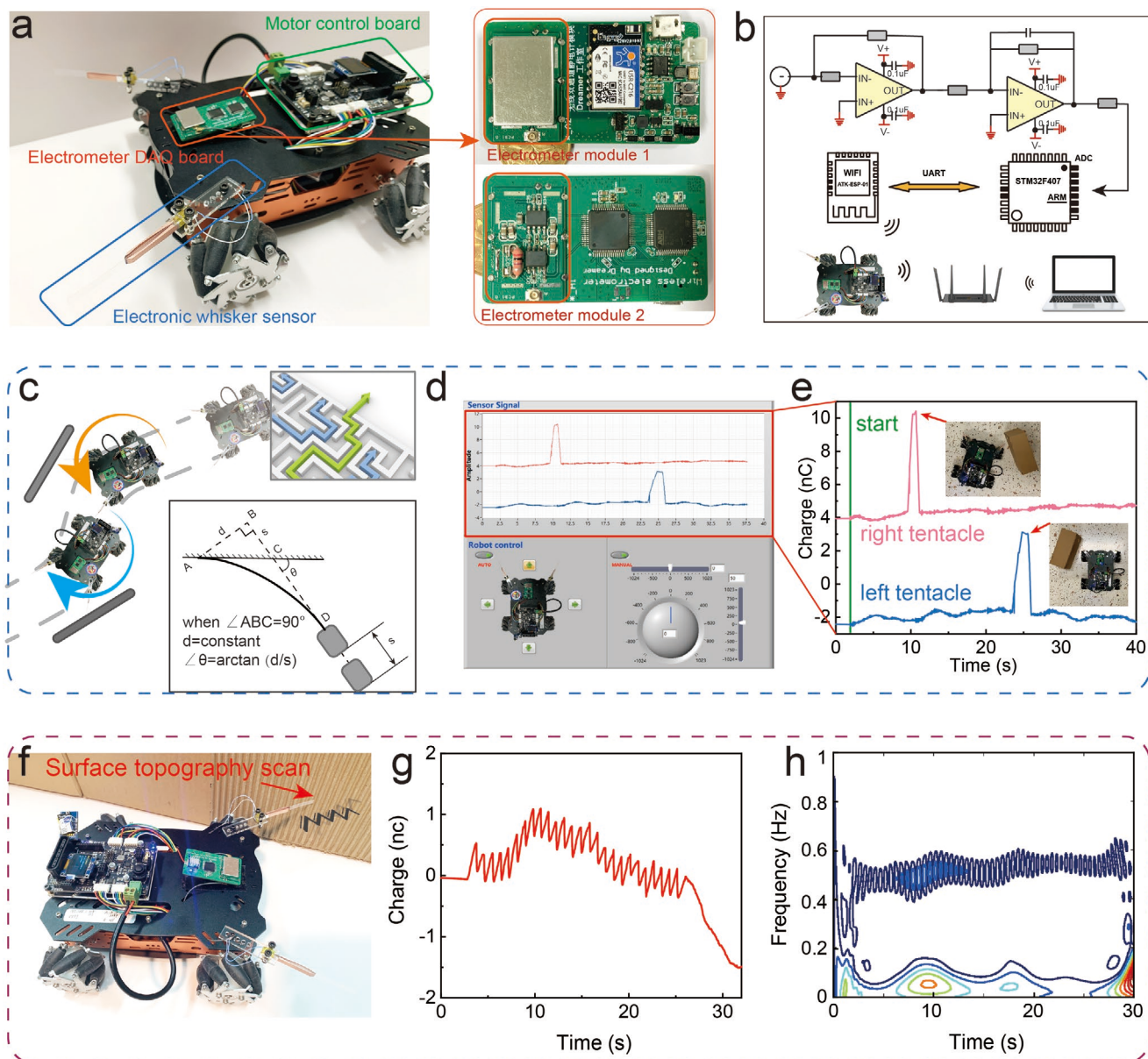


Figure 4. Application demonstration of the BWMR in robotics for environment and obstacle recognition as well as object surface topography scan. a) Photograph of the automated guided vehicle (AGV) equipped with a BWMR system, made of a group of BWMR sensors and an electrometer DAQ board. There are two electrometer modules on this board to acquire the charge signals from the right and left BWMR sensors, respectively. b) Schematic diagram of the electrometer DAQ board and AGV system. c) Strategy and trajectory, d) automated control program, and e) real-time acquired transferred charge signals from the electrometer DAQ board in the process of autonomous obstacle avoidance. The inset of (c) is the schematic diagram of acquisition method of collision angle, and the insets of (e) are the state photographs of the robot when it touches obstacles. f) Photograph of the robot car, g) acquired surface topography data, and h) the signal after pseudo Wigner–Ville transformation during the scanning process for object surface topography.

(Figure 5b and Figure S9 and Note S6, Supporting Information), the mimetic robot equipped with BWMR can perceive the movement of surrounding object by detecting the vibrational waves of the ground. By analyzing the amplitude and frequency of the shock waves, the robot can roughly identify approaching object and locate the vibration position, so as to catch prey and avoid danger like a spider (Figure 5c–e and Video S2, Supporting Information). Relying on the tactile receptors in the legs, spiders can also walk on complex road surface such as leaves without falling (Figure 5f). Similar ability is endowed

with robots by the BWMR. The pressure applied on its feet during walking can be sensed by the biomimetic robot in real time, so if the ground is not touched, the robot can change the course of movement to prevent falling. We demonstrated the real-time acquisition of foot pressure during the walking process of the robot in Figure 5g,h and Video S3, Supporting Information. Real-time feedback of the foot pressure can help robot analyze its gait and ground environment information which is beneficial for passing through complex roads efficiently. There are still many abilities that can be developed and explored,

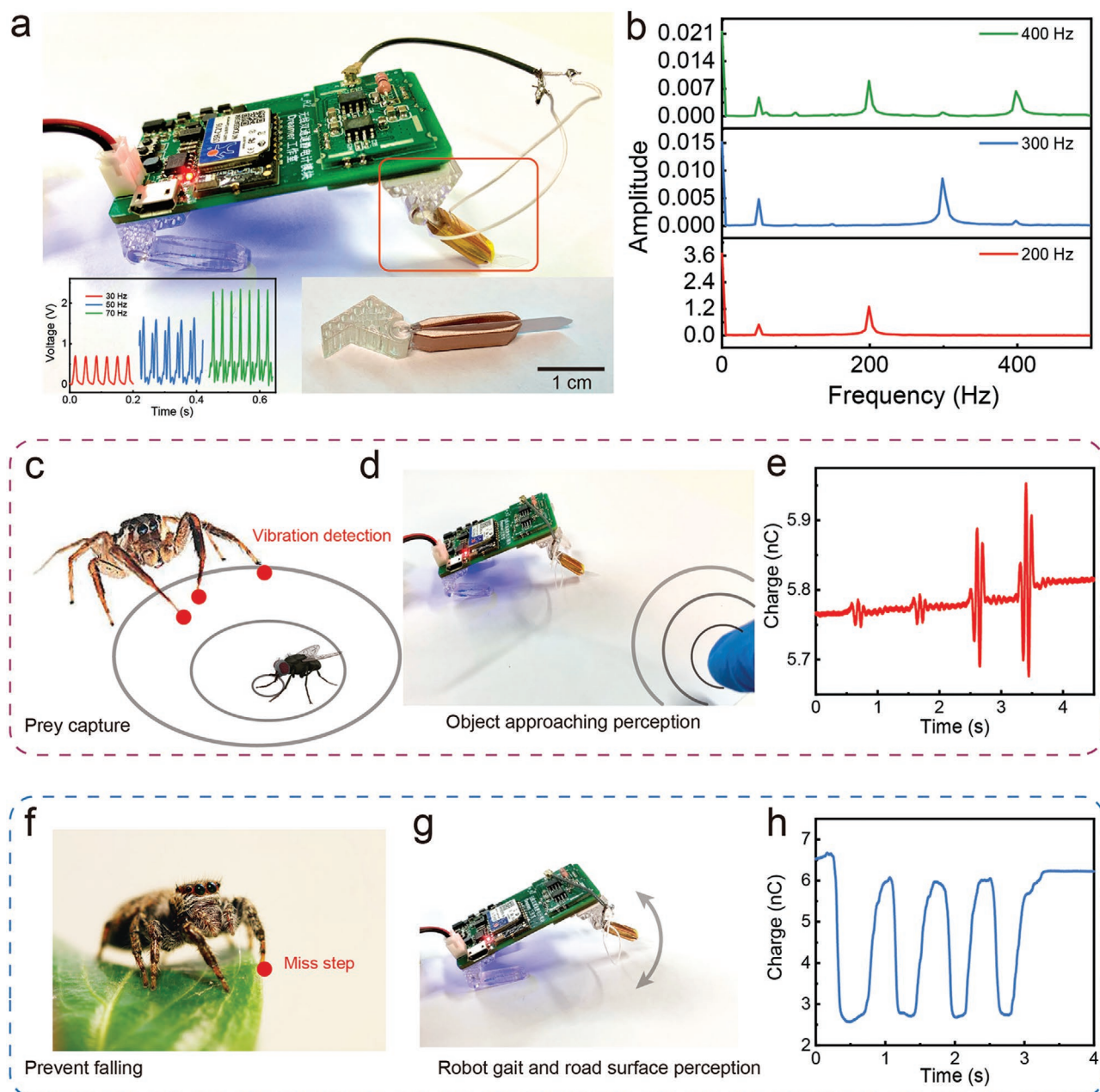


Figure 5. Application demonstration of the BWMR in robotics for vibration detection and road condition perception. a) Photograph of the quadruped robot equipped with a BWMR system, consisting of a BWMR sensor and an electrometer DAQ board acting as the leg and body, respectively. The inset shows the response character to vibration frequency and the enlarged view of robot leg. b) Spectrogram of voltage signals collected by the BWMR when vibrations with different frequencies are applied on the whisker. c) Schematic illustration of a spider using the vibration receptors on its feet to capture prey. d) Photograph of a biomimetic robot perceiving approaching objects and e) real-time acquired signals by the BWMR. f) Photograph of a spider preventing falls by sensing the pressure on its feet. g) Photograph of biomimetic robot perceiving its working gait and road surface condition, and h) real-time acquired signals when the robot walks.

thanks to the tactile sensory system, and the BWMR endows the robot with versatile functions.

2.6. Application in Mechatronic Instrument

In addition to applications in the field of robotics, BWMRs can also play an important role in industrial systems, due to

its excellent stability and sensitivity characteristics. Traditional mechanical indicators are widely used in industry due to their stable and easy troubleshooting characteristics. However, it is hard to realize intellectualization without electrical signals. Here one of the applications of the BWMR is demonstrated in gauges as an indicating pointer to realize parameter (such as pressure, mileage, and flow) direct indication and remote transmission by detecting its rotation angle (Video S4, Supporting

Information). Through reasonable structural design, the BWMR can also find applications in electromechanical indication and sensing of angle, displacement, height, and other mechanical parameters, for its versatile characteristics.

A set of meter-based remote monitoring system is constructed by integrating the pressure gauge with the BWMR pointer, a wireless electrometer module, and computer program (Figure 6a and Figure S10, Supporting Information). When

the pressure changes, the pointer will rotate along the central point and generate a series of peak signals when passing across the surrounding scales. The electrometer module collects the signals generated by the BWMR and sends them to the computer program through the wireless transmission for the next signal analysis and processing. First, the computer program filters the received signal to remove the environmental noise. Second, the differential algorithm differentiates the signal and

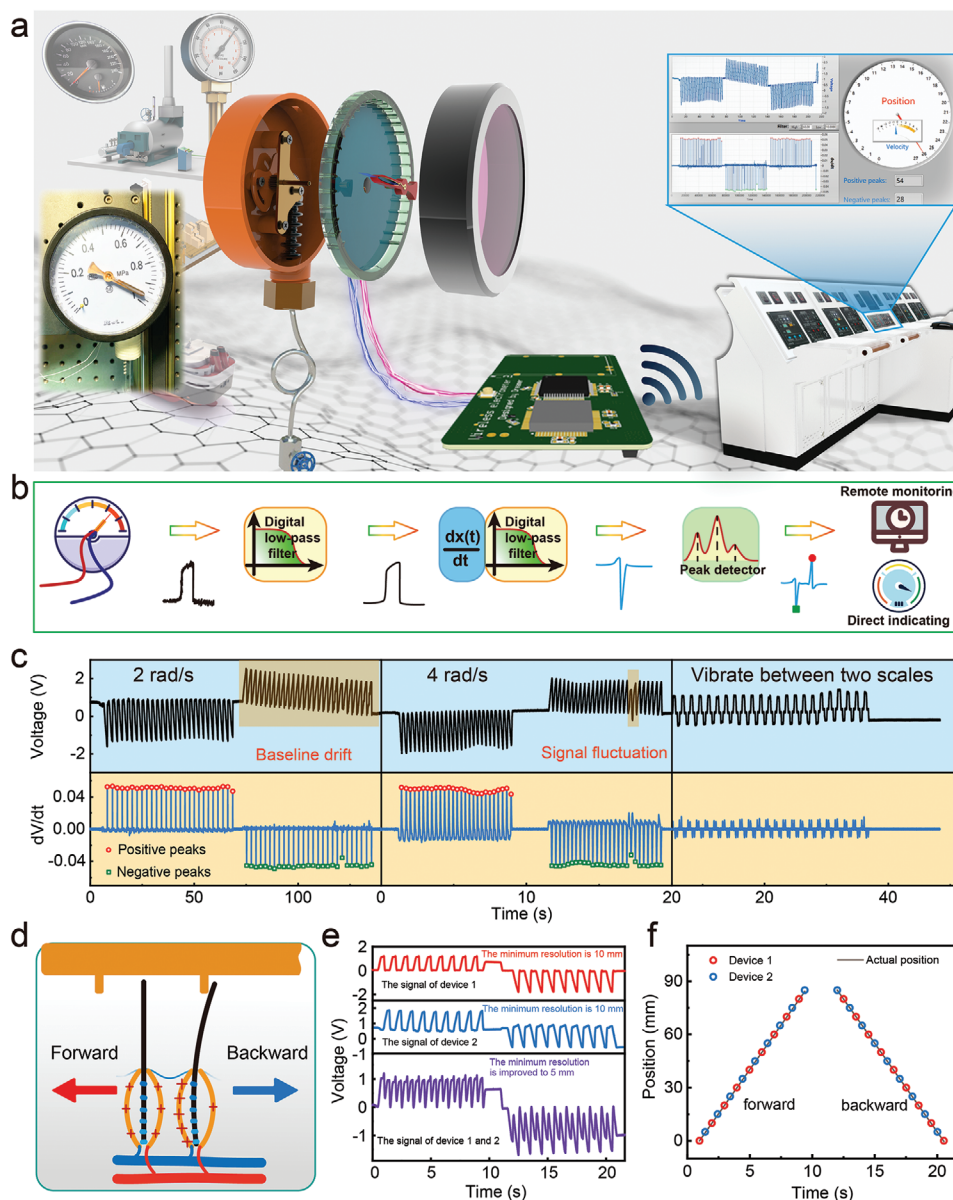


Figure 6. Application of the BWMR in the industrial field for direct displaying and remote monitoring of key parameters. a) Schematic illustration of mechatronic indication system for remote monitoring and direct displaying of speed, pressure, and displacement. b) Schematic diagram of mechatronic meter with the BWMR pointer for remote acquisition of its rotation angle. After filtering and differentiation, the numbers of negative and positive peaks of dV/dt profiles can be counted to acquire the pointer position. c) The V_{OC} and dV/dt variations of the BWMR meter when the pointer rotates at different speeds and vibrates between two scales. The positive and negative peaks are respectively the clockwise and counterclockwise rotation signals. There are a baseline drift and signal fluctuation in the voltage signals, but after differential processing, the signals are more stable and have higher anti-interference ability. d) Schematic illustration of resolution improved by utilizing more than one BWMR pointer. e) The V_{OC} signals from pointer 1, pointer 2, and two pointers connected in parallel. The peak density is doubled by utilizing two BWMR pointers. f) Calculated pointer position according to the signal peak numbers of two parallel devices, compared with actual values.

filters it again to obtain a purer dV/dt signal. Third, the peak numbers of the dV/dt signal are obtained through the peak monitoring algorithm. Finally, the number of impacted scales and the corresponding pressure value are derived (Figure 6b). The differentiated signal has strong anti-interference ability, thanks to the effective elimination of baseline drift caused by environmental interference, which ensures the accurate extraction of the pulse peak. Figure 6c illustrates the voltage and dV/dt signals obtained after processing when the pointer rotates at the speeds of 2 and 4 rad s^{-1} , and vibrates between two scales. The red and blue points correspond to the positive and negative peaks recognized by the program, respectively. Even when the pointer swings between two scales to produce mechanical noise due to the environmental vibration, the identification of signal peaks will not be affected. Indeed, sufficiently strong dV/dt peaks can only be generated when the pointer completely crosses a scale.

The resolution rate can be enhanced by increasing the density of scales as described in Figure 2, since the minimum resolution is equal to the distance between two scales for one BWMR sensor. But in some occasions, increasing the density of the scales is difficult and can also greatly increase the production cost. The resolution can also be improved by connecting multiple sensors in parallel as illustrated in Figure 6d and Figure S11, Supporting Information. For example, if the scale is x mm, the generation of a signal peak needs the sensor to move on x mm when using a single BWMR, and the corresponding minimum resolution is x mm. However, if γ BWMRs are connected in parallel as a whole sensor with the distance of x/γ mm between two adjacent ones, the sensor only needs to travel a distance of x/γ mm in order to generate a peak signal, and the corresponding resolution is improved by γ times. As presented in Figure 6e,f, the signals produced by the sensor with two BWMRs connected in parallel are the result of the superposition of the signals generated by each of them, double-peak signals. The corresponding resolution for position is improved and reaches 5 mm.

3. Conclusion

A BWMR based on the structural and functional bionics design of animal's whisker mechanoreceptors is proposed and investigated for robotic tactility in this work, which exhibits merits of easy fabrication, low cost, high sensitivity, and stability. Owing to its energy conversion ability from the TENG technology, no additional electric power supply is required for the BWMR, greatly promoting its distributed applications in robotics. The extruded whisker contributes to distinguishing weak environmental disturbances of 1.129 μN by its leverage effect, which endows the robots with sensitive tactile ability for environmental detection, with effectively improved device lifetime, stability and anti-interference performance compared to electronic skin. Furthermore, a tactility system is constructed by integrating BWMR and wireless electrometer DAQ circuit. By adopting the peak-counting strategy, a real-time mechatronic indication system has been demonstrated for direct parameter indication and remote synchronous monitoring in industrial equipment with high reliability and stability. A robotic tactile sensing system has also been conceived and assembled to dem-

onstrate its function in robotics for environmental recognition, object surface topography collection, surrounding object and ground environment detection, and self-gait analysis. The structure, dimension of the BWMR, and its signal acquisition method can be further improved in future works. The BWMR is promising for being developed into a multifunctional perturbation receptor array like animal's whisker and bristle, which could be widely employed in environmental monitoring, parameter indication, and sensing for industrial equipment, as well as tactile technology for robotic navigation, prey-tracking, and danger avoidance.

4. Experimental Section

Fabrication of the Biomimetic Whisker Mechanoreceptor: The BWMR was composed of two main parts, that is, the whisker and the artificial hair follicle. The chosen material for the whisker body was a strip of FEP film with a thickness of 0.2 mm, whose surface was etched by the ICP technique followed by hot pressing to make it straight. The etching gas was a mixture of O_2 and Ar gases with a ratio of 95:5. A power source of 400 W for generating plasma and a power of 100 W for accelerating the plasma ions were used. The etching time was set to be 60 s. The artificial hair follicle was fabricated by cutting the acrylic boards into designed shapes, and the structural sketches can be found in Figure S2, Supporting Information. The inner walls on both sides of the chamber were spray-coated with copper metallic paint, and cured at room temperature for 4 h to function as two electrodes of TENGs for sensing the deformation of whisker. In the assembly process, the root of whisker was inserted into the chamber before the chamber was sealed by two lids and silica gel (Figure S12, Supporting Information).

Characterizations and Measurements: The BWMR sensor and mechatronic meter was driven by a linear motor system (J-Best Corporation) for the characterizations. The moving speed and distance could be controlled from the computer in real time. A programmable electrometer (Keithley 6514) was used to measure the open-circuit voltage, and the acquired data were collected by DAQ program through a signal adaptor (J-Best Corporation). In the pressure sensitivity characterization process, the pressure applied on the whisker was acquired by a pressure gauge (MARK-10) with a resolution of 0.1 mN. The electrical signals and pressure signals from the electrometer and pressure gauge were acquired synchronously by the computer program constructed on the basis of LabVIEW (Figure S13, Supporting Information). The stability test was performed by using liner motor to drive the BWMR to slide back and forth across the 100 mm long scale at a speed of 10 mm s^{-1} . This process lasts for 4000 s (Figure S14, Supporting Information). Field-emission scanning electron microscopy (Hitachi SU8020) was applied to investigate the surface morphology of etched nanostructures on the surface of the FEP film.

Fabrication of Electrometer Data Acquisition Board and Autonomous Obstacle Avoidance System: The electrometer circuit was equipped to acquire the transferred charge signals of the BWMR, which was beneficial relative to acquiring the voltage due to the limited charges of TENG. The acquired analog signals by the electrometer circuit were transferred to digital signals by analog-to-digital converter, and sent to the microcomputer (STM32F405) for processing and calculation. The calculated signals were finally transmitted to the computer program through a WIFI module (USR-C216) for final analysis and decision making.

The autonomous obstacle avoidance system was composed of a car with Mecanum wheels, the BWMR tactile sensory system, and a remote-control program. The program got the surrounding environmental information and status of the car by analyzing the acquired BWMR signals in real time, and controlled the car to avoid obstacles by sending control messages to drive the circuit board of the car.

Fabrication of Quadruped Robot and Object Approaching Detection System: The legs of robot were fabricated by 3D printing, each of which

consists of a BWMR to sense the pressure of feet. The electrometer DAQ board functioned as the body of robot with four legs stick on it. The BWMR was connected to the signal input port of electrometer DAQ board for sending acquired signal to computer program in real time.

Mechatronic Meter and Mechatronic Indication System: The mechatronic meter body was a commercial pressure gauge, but the pointer was replaced by the BWMR sensor. The rotation was driven by inner gear mechanism to simulate the external pressure changes. A conductive slip ring was used to bring out the signal from the BWMR pointer, so that the wires would not be entangled due to the rotation of pointer. The acrylic circular dial was made by the laser cutting with the uniform scale of 8.83°.

The mechatronic meter, electrometer DAQ board, and computer program made up the mechatronic indication system. The electric signals generated during the rotation process of the meter pointer were acquired by the electrometer DAQ board and transmitted to the computer program to realize remote monitoring of key parameters. The program was designed based on the platform of LabVIEW, which could calculate and acquire the pointer positions according to the positive and negative peak numbers of signals.

Supporting Information

Supporting Information is available from the Wiley Online Library or from the author.

Acknowledgements

J.A., P.C., and Z.W. contributed equally to this work. This work was supported by the National Key R & D Project from Minister of Science and Technology (2016YFA0202704) and National Natural Science Foundation of China (Grant No. 51702018, 51432005, and 51561145021), and sponsored by CAS-TWAS President's Fellowship for international students. The authors also thank Yidan Wang for the design of some schematic diagrams in this paper.

Conflict of Interest

The authors declare no conflict of interest.

Data Availability Statement

Research data are not shared.

Keywords

biomimetic hairy whiskers, self-powered sensors, robotic tactility, triboelectric nanogenerators

Received: March 9, 2021

Revised: March 27, 2021

Published online:

[1] B. Siciliano, O. Khatib, *Springer Handbook of Robotics*, Springer International Publishing, Berlin, Germany **2016**.

[2] a) M. Vagaš, M. Hajduk, J. Semjon, L. Koukolová, R. Jánoš, *Adv. Mater. Res.* **2012**, 463–464, 1711; b) B. Mazzolai, C. Laschi, *Sci. Rob.* **2020**, 5, eaba6893.

- [3] Y. Yang, J. Chen, J. Engel, S. Pandya, N. Chen, C. Tucker, S. Coombs, D. L. Jones, C. Liu, *Proc. Natl. Acad. Sci. USA* **2006**, 103, 18891.
- [4] K. Pohlmann, F. W. Grasso, T. Breithaupt, *Proc. Natl. Acad. Sci. USA* **2001**, 98, 7371.
- [5] K. S. Severson, D. Xu, H. D. Yang, D. H. Oconnor, *eLife* **2019**, 8, e41535.
- [6] a) M. Asadnia, A. G. P. Kottapalli, J. Miao, M. E. Warkiani, M. S. Triantafyllou, *J. R. Soc., Interface* **2015**, 12, 20150322; b) X. Zhang, X. Shan, T. Xie, J. Miao, H. Du, R. Song, *Measurement* **2021**, 172, 108866.
- [7] E. Hittinger, P. Jaramillo, *Science* **2019**, 364, 326.
- [8] a) C. Wu, A. C. Wang, W. Ding, H. Guo, Z. L. Wang, *Adv. Energy Mater.* **2019**, 9, 1802906; b) F.-R. Fan, Z.-Q. Tian, Z. L. Wang, *Nano Energy* **2012**, 1, 328.
- [9] a) C. Zhang, W. Tang, C. B. Han, F. R. Fan, Z. L. Wang, *Adv. Mater.* **2014**, 26, 3580; b) Z. L. Wang, J. Chen, L. Lin, *Energy Environ. Sci.* **2015**, 8, 2250.
- [10] a) W. Xu, H. Zheng, Y. Liu, X. Zhou, C. Zhang, Y. Song, X. Deng, M. Leung, Z. Yang, R. X. Xu, Z. L. Wang, X. C. Zeng, Z. Wang, *Nature* **2020**, 578, 392; b) P. Chen, J. An, S. Shu, R. Cheng, J. Nie, T. Jiang, Z. L. Wang, *Adv. Energy Mater.* **2021**, 11, 2003066; c) H. Wang, L. Xu, Y. Bai, Z. L. Wang, *Nat. Commun.* **2020**, 11, 4203; d) Z. L. Wang, T. Jiang, L. Xu, *Nano Energy* **2017**, 39, 9; e) Z. L. Wang, *Nature* **2017**, 542, 159; f) J. Chen, Y. Huang, N. Zhang, H. Zou, R. Liu, C. Tao, X. Fan, Z. L. Wang, *Nat. Energy* **2016**, 1, 16138; g) Y. Zou, P. C. Tan, B. J. Shi, H. Ouyang, D. J. Jiang, Z. Liu, H. Li, M. Yu, C. Wang, X. C. Qu, L. M. Zhao, Y. B. Fan, Z. L. Wang, Z. Li, *Nat. Commun.* **2019**, 10, 2695.
- [11] a) T. Jin, Z. Sun, L. Li, Q. Zhang, M. Zhu, Z. Zhang, G. Yuan, T. Chen, Y. Tian, X. Hou, C. Lee, *Nat. Commun.* **2020**, 11, 5381; b) J. Luo, Z. Wang, L. Xu, A. C. Wang, K. Han, T. Jiang, Q. Lai, Y. Bai, W. Tang, F. R. Fan, Z. L. Wang, *Nat. Commun.* **2019**, 10, 5147; c) X. J. Pu, H. Y. Guo, J. Chen, X. Wang, Y. Xi, C. G. Hu, Z. L. Wang, *Sci. Adv.* **2017**, 3, e1700694; d) X. Peng, K. Dong, C. Ye, Y. Jiang, S. Zhai, R. Cheng, D. Liu, X. Gao, J. Wang, Z. L. Wang, *Sci. Adv.* **2020**, 6, eaba9624; e) H. Guo, X. Pu, J. Chen, Y. Meng, M.-H. Yeh, G. Liu, Q. Tang, B. Chen, D. Liu, S. Qi, C. Wu, C. Hu, J. Wang, Z. L. Wang, *Sci. Rob.* **2018**, 3, eaat2516; f) Y. C. Lai, J. Deng, R. Liu, Y. C. Hsiao, S. L. Zhang, W. Peng, H. M. Wu, X. Wang, Z. L. Wang, *Adv. Mater.* **2018**, 30, 1801114.
- [12] J. Chen, Z. L. Wang, *Joule* **2017**, 1, 480.
- [13] W. Li, D. Torres, R. Diaz, Z. J. Wang, C. S. Wu, C. Wang, Z. L. Wang, N. Sepulveda, *Nat. Commun.* **2017**, 8, 15310.
- [14] J. An, Z. Wang, T. Jiang, P. Chen, X. Liang, J. Shao, J. Nie, M. Xu, Z. L. Wang, *Mater. Today* **2020**, 41, 10.
- [15] Z. Wang, J. An, J. Nie, J. Luo, J. Shao, T. Jiang, B. Chen, W. Tang, Z. L. Wang, *Adv. Mater.* **2020**, 32, 2001466.
- [16] a) C. Wang, C. Pan, Z. Wang, *ACS Nano* **2019**, 13, 12287; b) Y. Kim, A. Chortos, W. T. Xu, Y. X. Liu, J. Y. Oh, D. Son, J. Kang, A. M. Foudeh, C. X. Zhu, Y. Lee, S. M. Niu, J. Liu, R. Pfattner, Z. N. Bao, T. W. Lee, *Science* **2018**, 360, 998; c) X. Pu, M. Liu, X. Chen, J. Sun, C. Du, Y. Zhang, J. Zhai, W. Hu, Z. L. Wang, *Sci. Adv.* **2017**, 3, e1700015; d) L. Chen, C. Wen, S.-L. Zhang, Z. L. Wang, Z.-B. Zhang, *Nano Energy* **2021**, 82, 105680.
- [17] K. J. Laboy-Juárez, T. Langberg, S. Ahn, D. E. Feldman, *Nat. Neurosci.* **2019**, 22, 1438.
- [18] a) H. Zou, L. Guo, H. Xue, Y. Zhang, X. Shen, X. Liu, P. Wang, X. He, G. Dai, P. Jiang, H. Zheng, B. Zhang, C. Xu, Z. L. Wang, *Nat. Commun.* **2020**, 11, 2093; b) H. Zou, Y. Zhang, L. Guo, P. Wang, X. He, G. Dai, H. Zheng, C. Chen, A. C. Wang, C. Xu, Z. L. Wang, *Nat. Commun.* **2019**, 10, 1427.
- [19] a) Z. L. Wang, *Mater. Today* **2017**, 20, 74; b) Z. L. Wang, A. C. Wang, *Mater. Today* **2019**, 30, 34; c) Z. L. Wang, *Nano Energy* **2020**, 68, 104272.